High-Resolution Fourier Diffraction at the IBR-2 Reactor

A. M. BALAGUROV
Frank Laboratory of Neutron Physics, JINR, 141980 Dubna, Russia

Introduction

High-resolution time-of-flight (TOF) diffractometers at short-pulse spallation neutron sources (SPS)—the most well-known example is HRPD at ISIS—have proved themselves to be extremely good for various applications. The resolution, $R = \Delta d/d$, close to 0.001 or even a bit better, can be easily obtained if a flight path amounts to 50-100 meters. But at so-called "long pulse sources" (LPS), with the pulse width Δt_0 equal to hundreds of microseconds, the flight path would need to be too long if a 0.001 resolution level is required. In this case, effective shortening of the neutron pulse should be done by employing a counter-rotating pair of fast disc choppers (see, for instance, Ref. [1]) or the correlation Fourier technique.

At present, several neutron Fourier diffractometers routinely operate and despite the fact that they have not earned a sufficiently good reputation yet, the results obtained with them show that the technique has been developed to a high degree of perfection and is competitive in various applications, especially in precise structural studies and residual stress measurements in bulk samples. Also, it seems that it is a fast Fourier chopper that would provide for the best compromise between today's highest $\Delta d/d$ resolution and intensity.

The IBR-2 pulsed reactor in Dubna is a LPS-type source with a pulse longer than 300 μs for thermal neutrons. Since 1995, the high resolution Fourier diffractometer HRFD [2] has been in routine operation at the IBR-2, and recently, the first diffraction patterns were measured at the second Fourier machine (FSD) intended for stress experiments at the IBR-2 [3]. In this paper, the current situation with HRFD (and, briefly, with FSD) is reported. In the beginning, some basic information about Fourier neutron diffractometry at an LPS-type source is given.

Fourier diffractometry at a pulsed neutron source

The general ideas of neutron Fourier diffractometry have been known since the late 1960s, but their successful practical realization became possible only in the 1980s after the so-called reverse time-of-flight (RTOF) method of data acquisition was introduced by Finnish physicists [4]. One after another, the mini-SFINKS [5] diffractometer in Gatchina, Russia, and the FSS instrument [6] in Geesthacht, Germany were constructed at steady state reactors. They both demonstrate the main advantage of the Fourier technique—a very high resolution at a very short flight path.

The main drawback of a Fourier diffractometer at a continuous neutron source is a high level of "correlation background" proportional to the total amount of the scattered neutrons and independent of the time of flight. For the first time, the situation with a Fourier chopper at a pulsed neutron source was analyzed in Ref. [**7**]. It was shown that, owing to additional time strobbing, the correlation background at a pulsed source is effectively suppressed, especially in the low-intensity parts of the incident spectrum.

As for any time-of-flight diffractometer, the resolution of HRFD depends on the TOF contribution and geometrical uncertainties. With the RTOF-method, the acquisition of the diffraction spectrum is performed at a continuously changing Fourier chopper frequency from zero to some upper value ω_m. In this case, the TOF component of the resolution function is close to Ω^{-1}, where $\Omega = N\omega_m$ is the maximum modulation frequency of the incident neutron beam, and N is the total number of transparent slits in the chopper. For $N = 1024$ and $\omega_m = 150$ Hz (HRFD parameters, maximum rotation speed $V_m = 9{,}000$ rpm), $\Omega^{-1} \approx 7$ μs. The geometrical contribution to the resolution function can be optimized by choosing an appropriate incident beam collimation and detector system to have a desirable level of resolution and intensity.

The transmission of the Fourier chopper is 0.25 because of a 0.5 open area and the triangular function of intensity modulation. There exists an additional decrease in the amplitude of a high-resolution diffraction peak due to the specifics of data acquisition by the RTOF method (ideally equal to 0.75, but is 0.2-0.4 in practice). In other words, in altogether equal conditions, the flux on the sample at the Fourier diffractometer is equivalent to ~0.10-0.05 of the flux at a conventional TOF diffractometer for the sample situated at the same distance from the source. In contrast to another correlation technique, the pseudorandom modulation of neutron beams, the Fourier method sets no limit on the neutron beam cross-section, which can be as large as is needed for good intensity until the resolution becomes worse due to large sample dimensions.

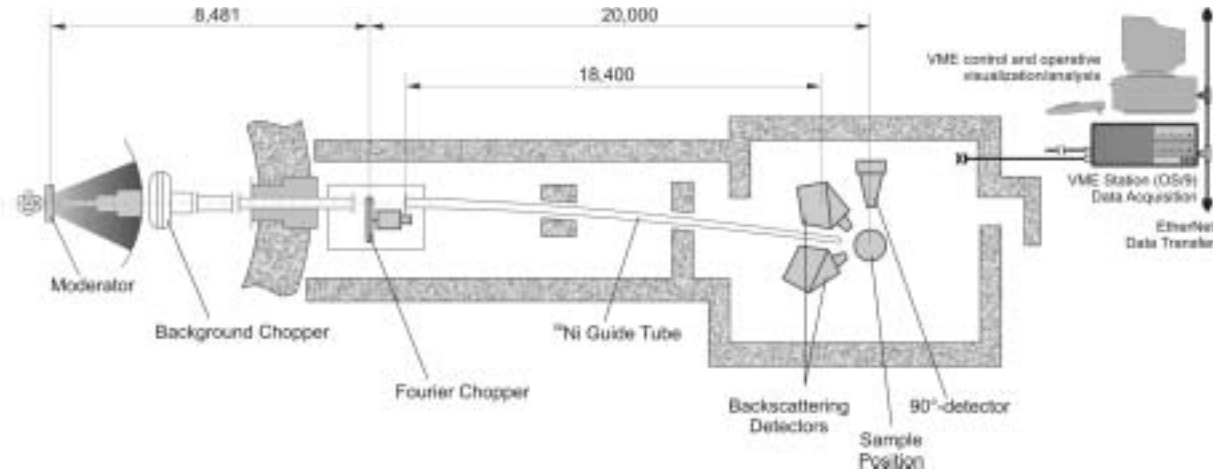

Figure 1. The layout of HRFD at the IBR-2 pulsed reactor.

HRFD at the IBR-2 pulsed reactor

A detailed description of the principles of the High Resolution Fourier Diffractometer (HRFD) operation, its design, and performance are presented in Ref. [2]. Functionally, the HRFD consists of the conventional components of any TOF-diffractometer (Figure 1). Additionally, the Fourier chopper is placed at a distance of ~9 m from the reactor core and at 20 m to the sample. At present, the total thermal neutron flux on the sample is about $3 \cdot 10^6$ n/cm^2/sec ($1.4 \cdot 10^7$ n/cm^2/sec without a Fourier chopper), and for the sample, ~2 cm^3 in volume; the data acquisition time is several hours. A typical high-resolution neutron diffraction pattern and the Rietveld refinement for a $(La_{0.1}Pr_{0.9})_{0.7}Ca_{0.3}MnO_3$ (LPCM-0.90) compound are shown in Figure 2.

From the dependence of the diffraction peaks width, W(d), on the maximal chopper speed, V_m, the TOF contribution can be determined and compared with calculations ($W_{TOF} = 58.5/V_m$, in μs if V_m is in 10^3 rpm). In Figure 3, one can see that the TOF contribution to the total width is indeed inversely proportional to the chopper speed. For $V_m = 11{,}000$ rpm, the W_{TOF} width is equal to 6.2 μs, and for $L = 30$ m and $d = 2$ Å, W_{TOF}/d could be as low as 0.0002, the value that is only achievable at synchrotron sources now.

The positive experience of the HRFD operation stimulated the construction of a new high-resolution Fourier Stress Diffractometer (FSD) at the IBR-2 pulsed reactor optimized for stress analysis in bulk materials [3]. The FSD design satisfies several requirements: high luminosity, high resolution, wide range of d_{hkl}, and fixed scattering angles $2\theta = \pm 90°$. In contrast to HRFD, in FSD, the flight path from chopper to sample position is only 5.5 m, which, nevertheless, assures $W_{TOF}/d \approx 0.0015$ for $d = 2$ Å. Another important FSD feature is a new type of detector with combined electronic-geometric focusing uniting a large solid angle and a small geometric contribution to the instrumental resolution: $\Delta d/d \approx 0.0023$ for back-scattering and ≈ 0.004 for 90°-detectors [8].

Examples of application

At present, HRFD is used for powder structure refinements, sometimes for experiments with single crystals if a very high d-spacing resolution is needed, and for residual stress measurements. In experiments with an $HgBa_2CuO_{4+\delta}$

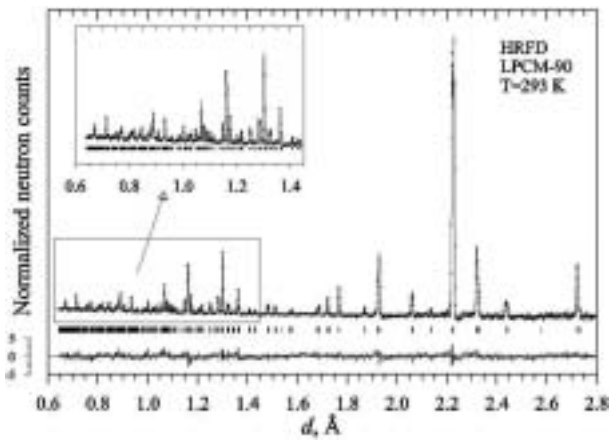

Figure 2. Diffraction pattern of the LPCM-0.9 sample measured at the HRFD at room temperature and treated with Rietveld method. The experimental points, calculated profile, and difference curve are shown. The difference is weighted by the mean-squares deviation for each point. Tics below the graph indicate the calculated peak positions.

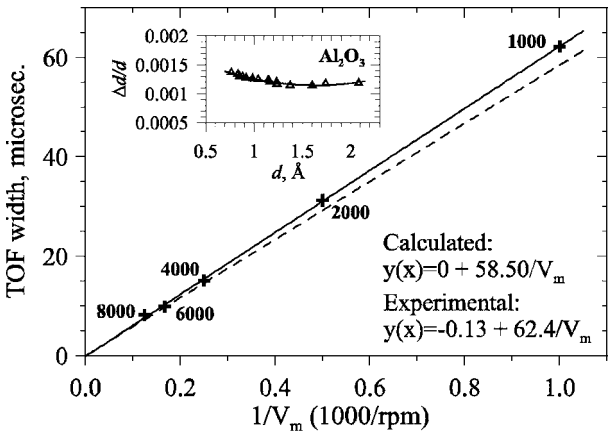

Figure 3. TOF contribution in the full width as a function of $1/V_m$. The points were measured at maximal Fourier chopper speed from 1000 to 8000 rpm. The least-square fit (continuous line) and calculated values (dashed line) are shown. In the insert, the relative width, $\Delta d/d$, of diffraction peaks, as a function of d-spacing, measured on an Al_2O_3 sample at maximal chopper speed of 8000 rpm is shown.

superconductor, structural results of principal importance have been obtained [9]. In the following study [10] of the fluorinated compound $HgBa_2CuO_4F_\delta$, the obtained neutron diffraction data showed twice the amount of extra fluorine in comparison with that for oxygenated Hg-1201 phases with similar T_c. This supports the ionic model of doping in Hg-1201: 2 holes per oxygen and 1 hole per fluorine. From a structural analysis of fluorinated Hg-1223, it was concluded [11] that the shortening of in-plane Cu–O distances at preserved (CuO_2) layers flatness in $HgBa_2Ca_2Cu_3(O/F)_{8+\delta}$ seems to be the main structural factor responsible for an enhancement of T_c up to 138 K, the highest transition temperature obtained at ambient conditions.

Another long series of experiments recently performed at HRFD have been connected with analysis of structural reasons for a giant oxygen $^{16}O/^{18}O$ isotope effect found in some CMR-manganites, especially in a $(La_{1-y}Pr_y)_{0.7}Ca_{0.3}MnO_3$ (LPCM-y) compound. The LPCM-0.75 composition offers a unique opportunity for a direct comparison of two structures: FM-metallic (sample with ^{16}O) and AFM-insulating (sample with ^{18}O). At room temperature and down to $T_C = 120$ K, both $^{16}O/^{18}O$ isotope-enriched samples have been found to be identical in crystal and magnetic structure, while at lower temperatures, their crystal structures are slightly different [12, 13]. The differences in the structural behavior of the O-16 and O-18 samples are clearly seen in Figure 4, where the temperature dependence curves of the <Mn-O> bond lengths and of the <Mn-O-Mn> valence angles are shown over the whole temperature range. The absolute values of the changes are very small; nevertheless, these two structures are definitely different. It is just this difference that could be the main reason for the coexistence of FM-M and AFM-I phases, which is often observed in doped manganites: Inhomogeneous stresses appearing on phase boundaries could stabilize the two-phase state [14].

While the main purpose of HRFD is powder diffraction studies, it is sometimes used for experiments with single crystals. For instance, it was employed in the experiment with a $La_2CuO_{4+\delta}$ single crystal when the macroscopic phase separation phenomenon at low temperatures was studied [15]. The diffraction evidence of phase separation can be seen clearly as the splitting of (*0k0*) peaks, which takes place at low temperatures (Figure 5). An analysis of the peak width as a function of d_{hkl} helped to determine the average size of the coherent domains of the coexisting phases as 975 ± 22 Å along the tetragonal axis and as 1460 ± 160 Å in the perpendicular direction. A joined neutron diffraction and μSR analysis of phase separation as a function of an extra oxygen content showed that it arises in parallel with superconductivity and is very likely driven by the formation of superconducting and AFM states [16].

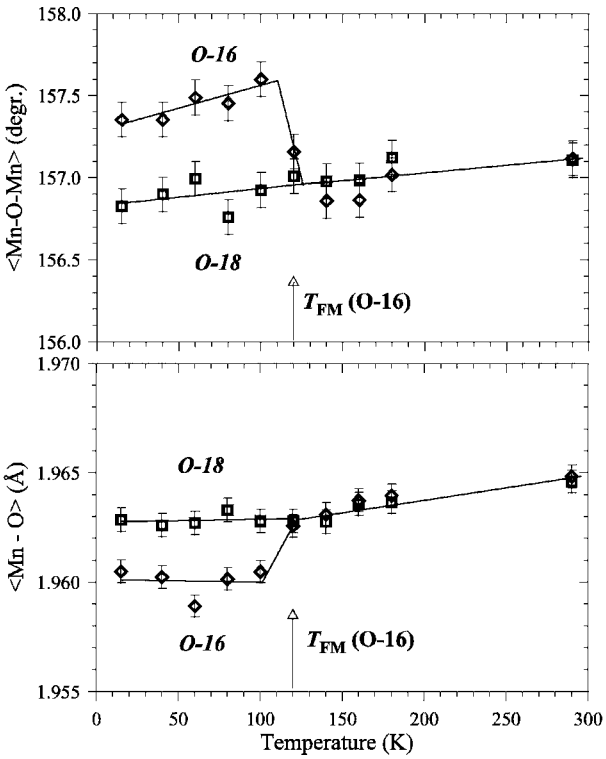

Figure 4. Comparison of the temperature dependencies of the average Mn-O bond lengths (in the bottom) and Mn-O-Mn valence angles for the LPCM-0.75 samples with ^{16}O and ^{18}O isotopes. The arrow indicates the temperatures of the phase transitions of the O-16 sample into FM metallic state. The lines are guides for the eye.

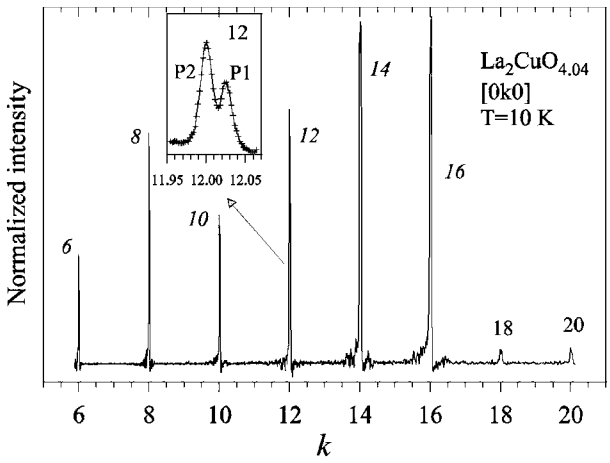

Figure 5. Diffraction pattern from the (010) plane for the $La_2CuO_{4.04}$ crystal measured at HRFD for 6th to 20th orders of reflection at 10 K. Figures denote the reflection orders. Each line is split, as shown for 12th order in the insert, due to crystal separation into the P1 (oxygen poor) and P2 (oxygen rich) phases.

From the very beginning of the HRFD operation, it was clear that it could be used for strain measurements in bulk samples. Indeed, in the last years, plenty of such experiments have been performed mainly in cooperation with the Fraunhofer Institute for Nondestructive Testing (Dresden) and the research institutions of the Russian Ministry of Atomic Energy (see, for instance, [17, 18]). But it is planned that after FSD completion, HRFD will be only used for structural experiments.

Conclusions

The Fourier diffractometer offers general advantages of the TOF technique and can be used both at steady state and pulsed neutron sources. In structural studies, when a wide *d*-spacing range is needed, the efficiency of the Fourier diffractometer is higher at high flux long pulse sources, such as the IBR-2 pulsed reactor or LPS-type spallation sources, which are planned for creation. The Fourier diffractometer, compared to a conventional TOF machine, ensures the obtainment of a very high resolution at a very short flight path, allowing the neutron flux to be increased and the cost of the instrument to be reduced. Also, it is important that its resolution can be easily varied continuously and within wide limits helping to optimize the diffraction experiment. The pulse overlapping is not important for the d_{hkl} range observed with the Fourier diffractometer; its influence is only on the level of the correlation background.

The HRFD is a noticeably more complicated machine than a conventional TOF-diffractometer. In addition to standard components, HRFD includes a Fourier chopper and a motor control system. For data acquisition, special correlation electronics based on digital signal processors are used. At the same time, the Fourier chopper is a much simpler and cheaper device than a high-speed Fermi chopper. Furthermore, it does not require synchronization of its rotation with the neutron source. The data collected with the Fourier diffractometer are analyzed in the same manner as those from a conventional TOF-machine. The only point requiring special attention is the peak shape, which has small negative depths on one or both sides of the diffraction peak. To take this into account, the so-called two-sign model of peak shape implemented in the MRIA program [19] is used.

Acknowledgments

All the work discussed in this paper is the result of the efforts of the many people at FLNP (Dubna), PNPI (Gatchina), MSU (Moscow), "Kurchatov Institute" (Moscow), VTT (Espoo, Finland), and IzfP (Dresden, Germany) named in the references. The work was partially financed under a JINR-BMBF (Germany) agreement.

References

1. F. Mezei, ICANS-XIII conference, *PSI Proceedings* **95-02**, I-400 (1995).
2. V. L. Aksenov, A. M. Balagurov, V. G. Simkin, A. P. Bulkin, V. A. Kudrjashev, V. A. Trounov, O. Antson, P. Hiismaki, and A. Tiitta, *J. of Neutron Research* **5**, 181 (1997).
3. G. D. Bokuchava, V. L. Aksenov, A. M. Balagurov, E. S. Kuzmin, V. V. Zhuravlev, A. P. Bulkin, V. A. Kudryashev, and V. A. Trounov *Applied Physics A*, **74**, S86 (2002).
4. H. Poyry, P. Hiismaki, and A. Virjo, *Nucl. Instr. and Methods* **126**, 421 (1975).
5. P. Hiismaki, V. A. Trounov, O. Antson, et al., Neutron scattering in the 'nineties, *Conf. Proc*., Vienna, IAEA, **453** (1985).
6. J. Schroder, V. A. Kudryashev, J. M. Keuter, et al., *J. of Neutron Research* **2**, 129 (1994).
7. P. Hiismaki, H. Poyry, and A. Tiitta, *J. Appl. Cryst*. **21**, 349 (1988).
8. E.S. Kuzmin, A. M. Balagurov, G. D. Bokuchava, V. V. Zhuk, V. A. Kudryashev, A. P. Bulkin, and V. A. Trounov, *J. of Neutron Research* **10**, 31 (2002).
9. V. L. Aksenov, A. M. Balagurov, V. V. Sikolenko, V. G. Simkin, V. A. Aleshin, E. V. Antipov, A. A. Gippius, D. A. Mikhajlova, S. N. Putilin, and F. Bouree, *Phys. Rev. B* **55**, 3966 (1997).
10. A. M. Abakumov, V. L. Aksenov, V. A. Alyoshin, E. V. Antipov, A. M. Balagurov, D. A. Mikhailova, S. N. Putilin, and M. G. Rozova, *Phys. Rev. Lett*. **80**, 385 (1998).
11. K. A. Lokshin, D. A. Pavlov, S. N. Putilin, E. V. Antipov, D. V. Sheptyakov, and A. M. Balagurov, *Phys. Rev. B* **63**, 064511 (2001).
12. A. M. Balagurov, V. Yu. Pomjakushin, D. V. Sheptyakov, V. L. Aksenov, N. A. Babushkina, L. M. Belova,

A. H. Taldenkov, A. V. Inyushkin, P. Fischer, M. Gutmann, L. Keller, O. Yu. Gorbenko, and A.R. Kaul, *Phys. Rev. B* **60**, 383 (1999).
13. A. M. Balagurov, V. Yu. Pomjakushin, D. V. Sheptyakov, V. L. Aksenov, N. A. Babushkina, L. M. Belova, O. Yu. Gorbenko, and A. R. Kaul, *Eur. Physical J. B* **19**, 215 (2001).
14. A. M. Balagurov, V. Yu. Pomjakushin, D. V. Sheptyakov, V. L. Aksenov, P. Fischer, L. Keller, O. Yu. Gorbenko, A. R. Kaul, and N. A. Babushkina, *Phys. Rev. B* **64**, 024420 (2001).
15. A. M. Balagurov, V. Yu. Pomjakushin, V. G. Simkin, and A. A. Zakharov, *Physica C* **272**, 277 (1996).
16. V. Yu. Pomjakushin, A. A. Zakharov, A. M. Balagurov, et al., *Phys. Rev. B* **58**, 12350 (1998).
17. G. Bokuchava, N. Shamsutdinov, J. Schreiber, and M. Stalder, *Textures and Microstr*. **33**, 207 (1999).
18. G. D. Bokuchava, A. V. Tamonov, N. R. Shamsutdinov, A. M. Balagurov, and D. M. Levin, *J. of Neutron Research* **9**, 255 (2001).
19. V. B. Zlokazov and V. V. Chernyshev, *J. Appl. Cryst*. **25**, 447 (1992).